The Influence of Temperature on the Magnetic Behavior of Colloidal Cobalt Nanoparticles

C. L. Dennis[1], G. Cheng[2], K. A. Baler[1], B. B. Maranville[1], A. R. Hight Walker[2], and R. D. Shull[1]

[1]Metallurgy Division, Materials Science and Engineering Laboratory, National Institute of Standards and Technology, Gaithersburg, MD 20899-8552 USA

[2]Optical Technology Division, Physics Laboratory, National Institute of Standards and Technology, Gaithersburg, MD 20899-8443 USA

Applications of magnetic nanoparticles, including hyperthermia for cancer treatments, require knowledge of how the colloidal environment affects the magnetic properties of the nanoparticles. Here, 10 nm diameter cobalt nanoparticles synthesized by thermodecomposition in 1,2-dichlorobenzene (DCB) are used to study the effect of the colloidal environment on the magnetic behavior of such materials. The magnetic properties are investigated by magnetization (M) versus temperature (T) measurements and vector magnetometry performed on the samples under zero-field-cooled conditions. Of particular interest in the M versus T data is a continuous rise in the magnetization observed around the DCB melting point during sample heating and a discontinuous drop around the DCB supercooling point during sample cooling. Vector magnetometer measurements quantify the portion of the sample that does not respond to the applied field. The magnitude of this unreversed component doubles with decreasing temperature as the temperature cools through the supercooling point in DCB. There is also an increase in the uniaxial anisotropy of the sample from $61.1(7) \times 10^{-7}$ J to $104.2(9) \times 10^{-7}$ J as the liquid-to-solid transition is traversed.

Index Terms—**Cobalt, magnetic anisotropy, magnetic nanoparticles, spin rotation.**

I. Introduction

RECENT advances in the chemical synthesis of magnetic nanoparticles with controllable size and shape are leading to new applications in a variety of fields, ranging from Coulomb blockade in single electron devices [1] and patterned media for magnetic data recording to biomedical applications like MRI contrast enhancers, DNA assays, and hyperthermia for cancer treatments [2]. In all of these applications, the environment of the nanoparticles affects their magnetic behavior and changes their effective shelf life. Therefore, it is necessary to understand how their colloidal and external (applied temperature, applied field) environment affect the magnetic behavior.

II. Experiment

A. Synthesis

The particles are synthesized by thermodecomposition of organo-metallic cobalt precursors in a boiling solvent, specifically 1,2-dichlorobenzene (DCB), by the method described previously [3] with one modification: dicobalt carbonyl is injected into DCB containing the surfactants oleic acid (OA) and trioctylphosphine oxide (TOPO) at a temperature of 120°C. After approximately 10 min, the temperature is raised to the reflux temperature of 180 °C and the synthesis is allowed to proceed for approximately 10 min before removal from the heat source. (See [4] or [5] for exact details of the synthesis.) The size and shape of these nanoparticles were characterized using transmission electron microscopy (TEM). A typical image of the particles (with an average diameter of 10.5 ± 1.0 nm) is shown in Fig. 1. Both selected area electron beam diffraction and X-ray diffraction performed on the nanoparticles confirmed that they are composed entirely of metallic Co in the ε-phase.

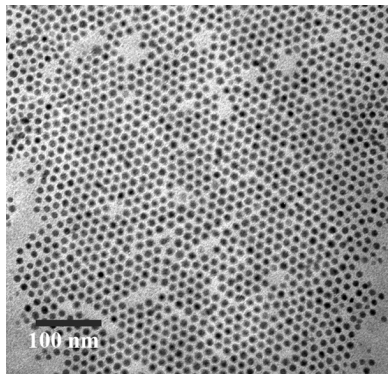

Fig. 1. Transmission electron micrograph of the 10 nm diameter Co nanoparticles as synthesized in 1,2-dichlorobenzene.

B. Magnetic Characterization

The magnetization versus temperature (M versus T) measurements were performed on both a superconducting quantum interference device (SQUID) magnetometer and on a vibrating sample magnetometer (VSM). The SQUID measurements used a variable field in a temperature range between 4.2 and 300 K, while the VSM measurements used a variable field and a temperature range between 150 and 300 K. The M versus T measurements were made after zero field cooling (ZFC) from 300 to 4.2 K, and then applying a field of $H = 15.9$ kA/m (200 Oe) prior to measuring the magnetization while warming and then cooling the sample. In addition, the SQUID measured the magnetization parallel to the applied field, while the VSM measured both the parallel and perpendicular components of the magnetization.

Digital Object Identifier 10.1109/TMAG.2007.893865

Color versions of one or more of the figures in this paper are available online at http://ieeexplore.ieee.org.

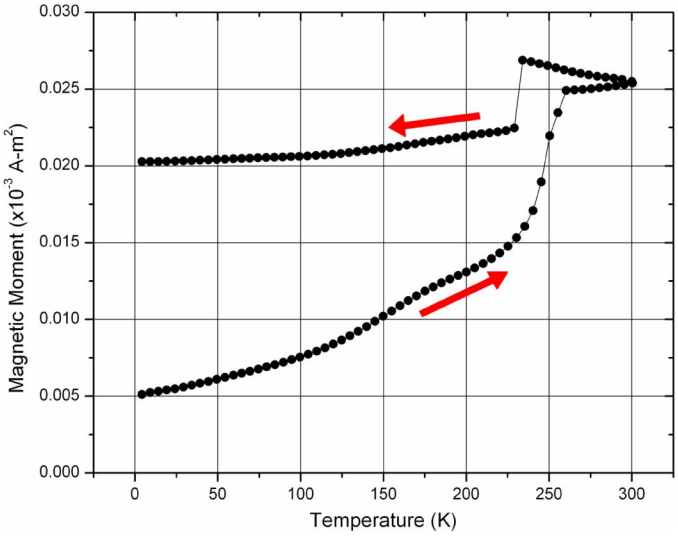

Fig. 2. Magnetization versus temperature characterization in $H = 15.9$ kA/m (200 Oe) after ZFC of 10 nm diameter Co nanoparticles as synthesized in 1,2-dichlorobenzene. The arrows indicate the direction of the measurement. (Note: M versus T of only DCB shows a purely diamagnetic signal.)

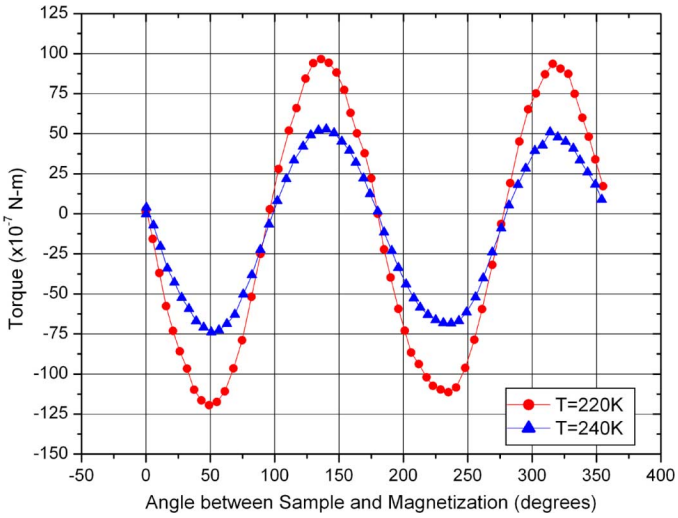

Fig. 3. Vector magnetometry measurements during cooling of the torque versus angle between the magnetization and a sample of 10 nm diameter Co nanoparticles as synthesized in 1,2-dichlorobenzene. The applied field was 1194 kA/m (15 000 Oe)—a saturated condition.

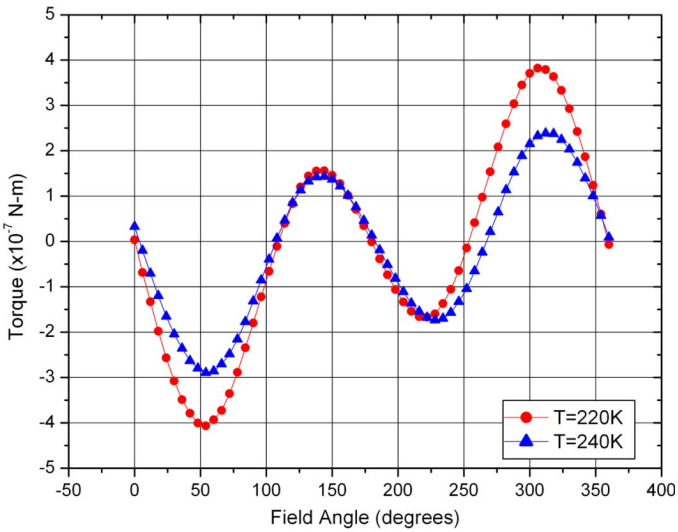

Fig. 4. Vector magnetometry measurements during cooling of the torque versus field angle of 10 nm diameter Co nanoparticles as synthesized in 1,2-dichlorobenzene. The applied field was 15.9 kA/m (200 Oe)—a nonsaturated condition.

C. Results and Discussion

1) Magnetization Versus Temperature Measurements: As previously described [4], [5], the as-synthesized Co in DCB nanoparticles are superparamagnetic at room temperature (298 K). At 5 K, below the blocking temperature ($T_B \sim 130$ K, as calculated based in the bulk anisotropy value for Co—see [4]), the sample is ferromagnetic with a coercivity of 65.8 kA/m (827 Oe). A detailed explanation of the M versus T measurements is provided in [4], so only the main ideas are mentioned here. As shown in Fig. 2, there is a continuous rise in the magnetization at $\sim$ 250 K during sample warming, and a discontinuous drop in the magnetization at $\sim$ 230 K during sample cooling. These temperatures correspond well to the differential scanning calorimetry analysis (see [4]) for the melting and supercooling points of the DCB. We hypothesize that the continuous rise is associated with a transition between two different spin rotation mechanisms: Néel rotation of the nanoparticles and/or chains at lower temperatures when the solvent is frozen and Brownian rotation of the nanoparticles and/or chains at higher temperatures when the solvent melts. We hypothesize that the discontinuous drop is due either to the exothermic reaction when the solvent supercools that provides enough thermal energy to slightly misalign the nanoparticles with respect to the field or to the competition between magnetic dipole alignment and lattice crystallization stresses. Both of these explanations are further corroborated [5] by the lack of these abrupt changes in magnetization in the dry sample, and by the shifting of the location of the continuous rise to correspond with the melting point of the new solvent when the solvent is changed. Furthermore, these continuous rises and discontinuous drops are completely reproducible [6]. Finally, the temperatures at which the continuous rise and discontinuous drop occurred were confirmed on the VSM to be the same (250 and 230 K, respectively), despite the inability of the VSM to go as low in temperature as the SQUID.

2) Magnetization Versus Angle: However, the question of interest in this investigation is the following: What is occurring magnetically around the discontinuous drop? To determine if the magnetization vector is changing as a function of temperature, the magnetization as a function of angle was measured with the VSM to obtain both the parallel and perpendicular components of the magnetization to the external field. The measurement protocol is as described in Section II-B, with results from along the cooling curve shown in Figs. 3 and 4.

These vector magnetometry measurements were made under two conditions: 1) in saturation ($H = 1\,194$ kA/m [15 000 Oe]) which quantifies the magnitude and type of anisotropy in the sample and 2) below saturation ($H = 15.9$ kA/m [200 Oe]) which mimics the actual conditions of the M versus T measurements. From the rotation VSM measurements at lower fields,

we cannot extract the anisotropy, but we can tell how much of the sample is rotating with the applied field.

To quantify the type and magnitude of the anisotropies in the sample, the torque data shown in Fig. 3 are fit to the following equation:

$$\tau = K_a \sin(2[\theta - \theta_A]) + K_d \sin(\theta - \theta_D) + C \qquad (1)$$

where τ is the torque on the system, K_a is the uniaxial anisotropy, K_d is the unidirectional anisotropy, θ is the angle, θ_A and θ_D are the offset angles for the uniaxial and unidirectional anisotropy respectively, and C is a constant offset. (For nanoparticles, the offset angles and offset constant are only fitting parameters; they have no physical meaning.)

Under saturation ($H = 1\ 194$ kA/m [15 000 Oe]), only a uniaxial anisotropy is present. (The unidirectional anisotropy is negligible at a constant value of 1.6×10^{-7} J.) These data are plotted in Fig. 3 as the magnetic torque versus the angle between the magnetization and the sample. (The sample angle is defined with respect to the initial magnetization direction.) When the sample magnetization is fully saturated ($M_S = 8.9 \times 10^{-5}$ A-m^2 [0.089 emu]), the torque is equal to the derivative of the magnetic energy with respect to the magnetization direction, and we can extract the magnetic anisotropy energy. At 240 K (after warming from 150 to 300 K and then cooling to just above the supercooling point of the DCB [$\sim$ 230 K]), the uniaxial anisotropy is $61.1(7) \times 10^{-7}$ J. After cooling through the solvent supercooling point from 240 to 220 K, the uniaxial anisotropy increases to $104.2(9) \times 10^{-7}$ J. This significant change in the anisotropy when crossing the liquid-solid phase transition is the result of turning the Brownian motion off. This locks the nanoparticles and their chains [7] into position, raising the anisotropy energy of any future adjustments.

For the second set of measurements ($H = 15.9$ kA/m [200 Oe]), no actual anisotropies can be determined because the sample is not in a saturated condition. Therefore, the data in Fig. 4 is plotted as a function of the field angle. The data can still be separated into its constituent harmonics: a $\sin(\theta)$ piece which represents the unreversed component of the magnetization and a $\sin(2\theta)$ piece which represents an effective anisotropy of the saturated nanoparticles. At 240 K (after warming from 150 to 300 K and then cooling to just above the supercooling point of the solvent), the first harmonic has a magnitude of 0.70 ± 0.03 while the second harmonic is 2.33 ± 0.03. After cooling through the solvent supercooling point from 240 to 220 K, the first harmonic has a magnitude of 1.65 ± 0.04 while the second harmonic is 3.04 ± 0.04. This change in the second harmonic indicates that there is also a slight increase in the effective anisotropy under the M versus T measurement conditions as the liquid-to-solid transition is traversed. These values are lower than those for the saturated case simply because not all of the nanoparticles are contributing. As for the first harmonic, this changes by a factor of 2.4 as the temperature cools through the supercooling point of the DCB, corresponding to a 2.4× increase in the magnitude of the unreversed component of the magnetization during traversal of the liquid-solid transition.

III. Conclusion

The uniaxial anisotropy of the sample increases from $61.1(7) \times 10^{-7}$ J to $104.2(9) \times 10^{-7}$ J as the DCB supercools, due to the inability of the nanoparticles and their chains to rotate. The existence of any anisotropy at 240 K is not, however, due solely to the presence of the chains, since there is no anisotropy present at 300 K. Instead, the DCB has partially frozen prior to the measurement, and these crystallites prevent the nanoparticles from responding to the field as they would in a liquid. This increase is also seen to a slightly lesser degree in the effective anisotropy (second harmonic) under nonsaturated conditions that more closely mirror that of the original M versus T measurements. Finally, the increase of the frozen-in component (first harmonic) with decreasing temperature implies that once the solvent is completely frozen, 2.4 times the number of nanoparticles get physically locked into their physical orientation and cannot rotate through Brownian motion to adjust to the changing field. Finally, in practice, these anisotropy changes may cause the heating characteristics of the nanoparticles to vary with temperature, resulting in variations in hyperthermia treatment efficacy.

Acknowledgment

The authors thank R. D. McMichael for useful discussions.

References

[1] Y. Xue and M. A. Ratner, "Nanomechanical modulation of single-electron tunneling through molecular-assembled metallic nanoparticles," *Phys. Rev. B*, vol. 70, pp. 155408–155413, Oct. 2004.

[2] Q. A. Pankhurst, J. Connolly, S. K. Jones, and J. Dobson, "Applications of magnetic nanoparticles in biomedicine," *J. Phys. D: Appl. Phys.*, vol. 36, pp. R167–R181, Jun. 2003.

[3] V. F. Puntes, K. M. Krishnan, and A. P. Alivisatos, "Colloidal nanocrystal shape and size control: The case of cobalt," *Science*, vol. 291, pp. 2115–2118, Mar. 2001.

[4] G. Cheng, C. L. Dennis, R. D. Shull, and A. R. H. Walker, "Influence of colloidal environment on the magnetic behavior of cobalt nanoparticles," *Langmuir*, submitted for publication.

[5] C. L. Dennis, G. Cheng, A. R. H. Walker, and R. D. Shull, "Environmental effects on the aging of colloidal cobalt nanoparticles," *J. Appl. Phys.*, submitted for publication.

[6] G. Cheng, C. L. Dennis, R. D. Shull, and A. R. H. Walker, "The influence of solvent freezing on the magnetic behavior of cobalt nanoparticles," unpublished.

[7] G. Cheng, D. Romero, G. T. Fraser, and A. R. H. Walker, "Magnetic-field-induced assemblies of cobalt nanoparticles," *Langmuir*, vol. 21, pp. 12055–12059, Dec. 2005.

Manuscript received October 31, 2006; revised February 21, 2007 (e-mail: cindi.dennis@nist.gov).